Materials Advances

ROYAL SOCIETY OF CHEMISTRY

PAPER

View Article Online
View Journal | View Issue

Cite this: *Mater. Adv.*, 2025, 6, 352

Development of titania coatings containing calcium, phosphorus, and silver, applied *via* the sol–gel method and dip-coating technique†

Karolína Opavová, *[a] Diana Horkavcová, [a] Eva Jablonská, [b] Lucie Mrázková[b] and Anna Bašusová[b]

Received 18th September 2024,
Accepted 4th December 2024

DOI: 10.1039/d4ma00941j

rsc.li/materials-advances

This research focuses on the development of titania coatings containing calcium, phosphorus, and silver, prepared using the sol–gel method and applied *via* dip-coating technique for use in biomedical implants. These coatings were evaluated for their adhesion, bioactivity, antibacterial properties, and cytocompatibility. The titanium substrates underwent mechanical grinding or blasting with Al_2O_3 particles, or chemical etching with hydrofluoric acid before coating application. Adhesion was assessed using a tape test, revealing that all coatings adhered well to the substrates. Antibacterial activity against *Escherichia coli* was evaluated after 4 and 24 hours, demonstrating significant antibacterial effects. Bioactivity was tested in simulated body fluid (SBF) over 20 days, showing promising results. Cytotoxicity was assessed using L929, U-2 OS, and hFOB 1.19 cell lines, confirming the biocompatibility of the coatings. These findings suggest that sol–gel prepared coatings can significantly enhance the functional properties of titanium-based biomaterials for biomedical applications.

Introduction

Surface treatments

Metal biomaterials and medical implants, crafted from materials such as stainless steel, titanium alloys, and cobalt alloys, are commonly used for their good biocompatibility and mechanical properties desired for load-bearing and dental applications.[1,2] Surface treatment techniques are used to enhance the durability and performance of biomedical substrates, and these treatments can improve their chemical, mechanical, and biological properties.[3] Numerous pieces of research show that surface roughness is an important parameter that affects the rate of osseointegration and fixation of implants. Techniques used to increase surface roughness and reaction surface area include machining, blasting, etching, and plasma spraying, among others.[4,5] Nowadays, various coating techniques are used as a highly efficient way to modify biomedical substrate surface, as it allows for the combination of material and coating properties. There are several methods for preparing functional coatings, like plasma spraying, electrochemical deposition, sol–gel, biomimetic deposition, sputtering, and others.[3,6,7]

Sol–gel

The sol–gel method is one of the most popular ways to prepare functional coatings. This simple and inexpensive chemical process based on hydrolysis and polycondensation reactions of precursors allows for the fabrication of multi-component materials in various forms (films, fibres, foams, *etc.*) from a liquid phase.[3,8–10] It has several advantages over other methods, including the possibility of doping various inorganic and organic materials, or biomolecules, the ability to create a uniform fine-grained structure, high homogeneity, excellent adhesion, and corrosion resistance. Additionally, it can coat substrates with a complex geometry and has a lower processing temperature. The sol–gel method is used not only in the biomedical field but also in optics (*e.g.* dielectric mirrors) or as anti-reflective coatings (ARCs).[3,9–11] Its cost-effectiveness and adaptability make it a practical choice for various industrial applications.[8,12]

Adhesion

Adhesion is an essential parameter in the study of coatings in the biomaterials field, as it determines their effectiveness and durability. Adhesion tests are used to assess the durability of coatings and determine if they are suitable for their intended

[a] *Department of Glass and Ceramics, Faculty of Chemical Technology, University of Chemistry and Technology Prague, Technická 5, 166 28 Prague 6, Czech Republic. E-mail: Karolina.Opavova@vscht.cz*
[b] *Department of Biochemistry and Microbiology, Faculty of Food and Biochemical Technology, University of Chemistry and Technology Prague, Technická 3, 166 28 Prague 6, Czech Republic*

† Electronic supplementary information (ESI) available. See DOI: https://doi.org/10.1039/d4ma00941j

purposes. Failure to adhere can cause many problems for the patient, including pain, infection and failure of the coating and the entire implant. There are several common and uncomplicated techniques for measuring bond strength, such as the *tape test*, scratch test, and pull-off test.[13–17]

Bioactivity

The term "bioactivity" has different definitions. Some define it as a specific biological response resulting in an interaction between a material and surrounding tissues, forming a bond. Others consider bioactive materials as capable of releasing ions and inducing bone hydroxyapatite formation in contact with physiological fluids.[18–20] According to the ISO 23317:2014 standard, bioactive materials are defined by their ability to form an apatite layer in simulated body fluid (SBF), which mimics the inorganic composition of human blood plasma, serving as a key indicator of their potential for bone bonding.[20] The bioactivity index $I_B = 100/t_{0,5}$ [d^{-1}] can be used to determine the bioactivity level, where $t_{0,5}$ is the time for 50% binding formation between the material and tissue.[21] Bioactivity is crucial for biomedical materials, enhancing their biocompatibility, osseointegration, and implant fixation. It triggers a specific biological response leading to stable tissue-implant bonds. The presence of calcium and phosphorus, with a ratio close to hydroxyapatite (Ca/P = 1.67), can increase bioactivity. Therefore, hydroxyapatite (HA) is a highly desirable bioactive material.[20,22–24]

Antibacterial effect

Bacterial resistance is very important, especially in clinical applications. Antibacterial materials are widely used to form antibacterial implant coatings, which protect substrates from bacterial contamination and prevent the formation of undesirable bacterial infections. Infections, in hospital environment mainly caused by *Escherichia coli* and *Staphylococcus aureus*, are a significant issue and risk during and after surgery. It may result in implant failure and subsequent reoperation. Maintaining a sterile environment allows for adequate tissue regeneration time and increases the chance of implant acceptance. In addition, the amount of antibiotics, which are a considerable burden for the patient's body, can be reduced.[25–28] One effective way to achieve antibacterial properties in implant coating is by incorporating silver nanoparticles or soluble compounds (*e.g.* $AgNO_3$, Ag_3PO_4). Silver has long been known for its antibacterial properties, and nanoparticles of silver have a large surface area relative to their volume, making them highly effective at killing different bacterial strains, viruses, and fungi. The gradual and long term release of silver from the biomaterial will provide a sufficient antibacterial effect.[22,28,29] The mechanism of action for silver is thought to involve the release of silver ions, which can penetrate bacterial cell walls and disrupt their metabolic processes.[23,29,30]

Cytotoxicity

The term cytotoxicity refers to the toxic effect of substances on cells. Cytotoxic agents prevent the growth of cells and sometimes cause their death. They are also used as a treatment for some diseases. There are chemical, biological, and physical agents that can affect cells to diverse degrees.[31] Medical devices and biomaterials are in direct and indirect contact with tissues and cells of a living organism and must exhibit excellent biocompatibility in addition to physical and chemical properties. Biocompatibility is essential in the field of biomaterials and medical technology. It is the ability of the material to perform the desired functions, induce an appropriate response of the organism, and interact with the living system without the risk of injury, toxicity, rejection of the implant by the immune system or any adverse reaction of the organism.[32,33] Biomaterials are often surface-modified with antibacterial coatings containing antiseptics, antibiotics, or metal ions, which prevent the colonization of the implant by microorganisms and the formation of a biofilm. While antibacterial properties are important, they should not compromise biocompatibility.[34]

Aims

The aim of this study was to prepare titanium coatings containing calcium, phosphorus, and silver on chemically and mechanically modified titanium substrates using the sol–gel method and dip-coating technique. Titanium was chosen due to its excellent biocompatibility and mechanical properties, which make it a widely used material in biomedical applications. The inclusion of calcium and phosphorus aims to enhance bioactivity and osteointegration, while silver was selected for its well-known antibacterial properties. This study provides new information to the current research by examining how different chemical and mechanical surface treatments influence the performance of the multifunctional coatings. The study aims to contribute to the development of advanced coatings that not only enhance the antibacterial and bioactive properties of titanium-based biomaterials but also ensure cytocompatibility. The findings from this research could significantly advance the field of biomaterials, providing valuable insights for future studies and potential clinical applications.

Experimental conditions

Substrate treatments

Titanium substrate samples (Grade 2, ASTM B265) sized 30 × 10 × 1 mm were prepared and subjected to three different surface treatments. The first group underwent mechanical treatment by grinding with SiC grinding papers (P400, P600 and P800). The second group was treated by blasting the samples with Al_2O_3 particles (90–125 μm; made by RONA, a.s. white fused alumina F120). The third group of samples underwent chemical treatment through etching in hydrofluoric acid ($HF:H_2O$, 1 : 5) for 20 seconds. Afterwards, all samples were cleaned in an ultrasonic bath using acetone and ethanol for 10 minutes each, followed by air-drying at laboratory temperature.

Sols preparation and coating

Three sols with varying concentrations of silver were prepared by mixing a basic titania sol with two 2 mol dm^{-3} ethanol solutions of calcium nitrate tetrahydrate (PENTA s.r.o.) and triethyl phosphate (Sigma-Aldrich s.r.o.). The basic sol was prepared by stirring a mixture of Triton X-100 (Carl Roth GmbH + Co. KG), nitric acid (1 mol dm^{-3}) (Lach-NER, s.r.o.), acetylacetone (Lach-NER, s.r.o.), tetra-*n*-butylorthotitanate (Sigma-Aldrich s.r.o.) and ethanol at laboratory temperature for 24 hours. This mixture was then combined with the ethanol solutions in the specified order and ratio (Ca/P = 1.67) and homogenized for an additional 24 hours. Silver in the form of $AgNO_3$ was introduced to the sols just prior to coating. The final concentrations of silver in the sols were 0 mol dm^{-3} (TCP), 0.05 mol dm^{-3} (TACP05), and 0.07 mol dm^{-3} (TACP07).

The three different coatings were applied to all three types of surface-treated titanium substrates by the dip-coating technique at laboratory temperature with constant stirring. The samples were submerged and extracted at a constant rate of 20 cm min^{-1}, and the dwell time in the sol was 30 seconds. Subsequently, the samples were dried at laboratory temperature and fired at 400 °C for 2 hours with a heating rate of 2 °C min^{-1}. This was followed by spontaneous cooling down to laboratory temperature.

Substrate surface morphology

The morphology and roughness of substrate surfaces after mechanical and chemical surface treatments, as well as those coated without silver content (TCP), were measured according to ČSN EN ISO standard 4287. Observation and characterization were made by using a 3D laser confocal microscope from Olympus (OLS5000-SAF). Roughness was measured and evaluated three times for each sample, using Data Acquisition Application and Analysis Application software.

Adhesion

The ability of the coatings to adhere to the surface-treated titanium substrates was tested by a standardized *tape test* (ASTM D 3359). The surfaces of the coatings were intentionally damaged with 6 × 6 grid scratches, with a 1 mm gap between each scratch. A special tape (Permacell 99) was applied to this grid and loaded for 90 seconds. Afterwards, the tape was peeled off at a 180° angle. After the *tape test*, the surfaces of the coatings were examined using an optical microscope (Olympus BX51) and a scanning electron microscope (Hitachi S4700). The final appearance of the coatings after the test was compared with a classification table to assign them a grade of adhesion.

Antibacterial effect

The antibacterial effect of coatings was tested against the Gram-negative bacteria *Escherichia coli*. The entire experiment was conducted in a sterile environment within a Flow-box. A test suspension with a concentration of 10^4 cells mL^{-1} was obtained by dilution of provided bacteria suspension with physiological solution (9 g L^{-1} NaCl). Each test tube contained a single coated sample immersed in the test suspension, while the reference samples consisted of tubes containing only the bacterial suspension. The interaction between the coated substrates and the bacterial suspension took place in the dark for 4 hours and 24 hours at laboratory temperature. After the interaction, the samples were withdrawn from the tubes, and 100 μL of each reacted suspension (as well as the reference unreacted suspension) were spread into two Petri dishes with agar. These dishes were incubated at 36.5 °C in a biological thermostat for 24 hours. After the incubation period, the Petri dishes were photographed, and the colonies of surviving bacteria were counted using the computer program NIS-Elements AR 3.10. The results of the antibacterial test are the average value from two independent experiments which means four Petri dishes.

Bioactivity

The bioactivity of the coatings was tested *in vitro* using simulated body fluid (SBF) under both static and static-dynamic conditions. The static test was performed according to ISO standard 23317:2014. The static-dynamic test differed in replacing the SBF every 24 hours, which better corresponds to the processes occurring in living organisms. Both tests lasted for 20 days. After the reaction time, the samples were removed from the solutions, rinsed three times in demineralized water, and air-dried at laboratory temperature. The sample surfaces after these tests were observed by a scanning electron microscope (Hitachi S4700) equipped with an EDS analyser (NORAN D-6823) with a silicon drift detector (SDD) and characterized with XRD analysis using a High Score Plus diffractometer equipment with a conventional X-ray tube (CuKα 40 kV, 30 mA) to determine the composition of newly formed phases. The samples were plated with an Au-Pd layer for SEM observation.

Cytotoxicity

Cytotoxicity testing *in vitro* was conducted using the mouse fibroblast cell line L929 (ATCC® CCL-1™) *via* test on extracts according to ISO 10993-5 standard, and by seeding the cells directly onto the samples (contact testing) with the use of U-2 OS cell line derived from human osteosarcoma (ATCC® HTB-96™) and with hFOB 1.19 cells derived from human fetal osteoblasts (ATCC® CRL-11372™). Cell viability was assessed by monitoring the transformation of blue resazurin into purple, fluorescent resorufin. Cells growing on the samples were observed using a fluorescence microscope.

For testing, full-coated samples of mechanically and chemically modified substrates were prepared and sterilized in 70% ethanol for two hours. Only samples coated with TCP and TACP07 were used due to the expected lower cytotoxicity in TACP05 coatings.

Test on extracts. To prepare extracts of the test samples, a Minimum Essential Medium (MEM, Sigma M0446) (surface-to-volume ratio of 1.25 cm^2 mL^{-1}) with a 5% FBS (Fetal Bovine Serum) and antibiotics was used. The extraction process took place for 24 hours at 37 °C with continuous shaking (130 rpm).

L929 cells were seeded in a 96-well plate in MEM + 10% FBS at a concentration of 1 × 10^5 cell mL^{-1}, aiming for sub-confluent

cell layers (approximately 80% of the well bottom was covered with cells), at the time of exposure. Cultivation occurred at 37 °C in an atmosphere with 5% CO_2 for 24 hours. Following this, the cell layer's growth was checked, and the medium was replaced by the extracts and another 24-hour incubation followed. The sole cultivation medium served as the negative control. Each extract was tested six times. After incubation, the extracts were removed and replaced with a solution of resazurin (final concentration 25 μg mL^{-1}) in a medium without phenol red (MEM + 10% FBS). Plates prepared in this manner were further incubated for 1 hour at 37 °C. The quantification of the resulting resorufin was performed by measuring fluorescence at excitation and emission wavelengths of 560 nm and 590 nm, respectively, using a Synergy H1 fluorometer. The evaluation was conducted by comparing the metabolic activity (fluorescence) of the samples to that of the negative control. In accordance with the established standards, cytotoxicity is considered to occur when cell viability decreases by more than 30% compared to the negative control. The concentration of silver in the extracts was determined using an ICP-OES iCAP 7400 (Thermo Scientific), and measurements were conducted only for samples coated with sol containing the higher Ag concentration (0.07 mol dm^{-3}; TACP07).

Direct contact cytotoxicity test and microscopy. For the contact test, the samples were sterilized and placed in 6-well plates, where 3 mL of cell suspension (U-2 OS 20.000 cells cm^2, hFOB 1.19 30.000 cells cm^2) in DMEM + 10% FBS + antibiotics were added to each sample. After 24 hours, the wells were washed with PBS (phosphate-buffered saline). The samples were then transferred to new wells. Subsequently, 2.5 mL of a resazurin solution in a medium without phenol red at a concentration of 25 μg mL^{-1} was added to the cells that were originally in contact with the samples. After a four-hour incubation, the amount of generated resorufin was measured again. Fluorescence measurement was conducted under the same condition as in the non-contact cytotoxicity testing, using a Synergy H1 fluorometer at excitation and emission wavelengths of 560 nm and 590 nm. Cells growing on the well bottom served as the negative control. Cells growing directly on the samples were fixed using a 4% formaldehyde solution in PBS (2.5 mL, 20 minutes) and permeabilized using a 0.1% Twen-20 (2.5 mL, 15 minutes). Cellular structures were visualized using TRITC-phalloidin (1 μg mL^{-1}, 12 minutes, for cytoskeleton visualization) and DAPI (0.5 μg mL^{-1}, 5 minutes, for nucleus visualization). The evaluation was performed using an Olympus BX53 fluorescence microscope with the CellSens Dimension software, and images were further processed in ImageJ software.

Results

Characterization of substrates

Fig. 1a–c show images of surfaces of non-coated titanium substrates treated in mechanical and chemical ways, depicted by a scanning electron microscope (Hitachi S4700). All surface-treatments of the substrate resulted in an increase in surface roughness and thus the increase of the reaction surface area. In the case of chemically treated samples, the hexagonal morphology of individual grains was accentuated.

The roughness of the surface-treated substrates was also measured using a 3D laser confocal microscope (Olympus OLS5000-SAF). By comparing the roughness profiles of surface-treated substrates, different morphology of the substrates was observed. The surface roughness of the substrate leached in the HF solution is not uniform, there are sudden jumps, on the other hand, the surface of the blasted substrate is very fragmented. The grinded surface is the most uniform of all samples.

Coatings characterization

Fig. 2a–i show the surfaces of the coatings after firing. An important part of coatings characterization was also the analyse of the coating's chemical composition by EDS, and coating roughness measurements. Fig. 3 presents a representative sample with an example of EDS analysis of the coating (Grinding TACP05), showing the distribution of selected major elements.

By observing the fired coatings, it was found that all types of coatings copied the surfaces of the surface-treated titanium substrate almost perfectly. In all types of coatings, isolated cracks throughout the surface emerged during the firing process. A significantly higher number of cracks were present in coatings on a blasted substrate, which might be attributed to substantial stress in areas of significant height difference.

Spherical "craters" containing calcium-rich particles appeared in all types of coatings, with sizes ranging from single to tens of micrometres. Their presence may result from an immiscible phase within the titania-phosphate/calcium nitrate system, leading to structural irregularities in the coatings. The distribution of these "craters" was notably influenced by the roughness and morphology of the substrate surfaces. The arrangement of these "craters" was more uniform on mechanically treated substrates compared to chemically treated ones.

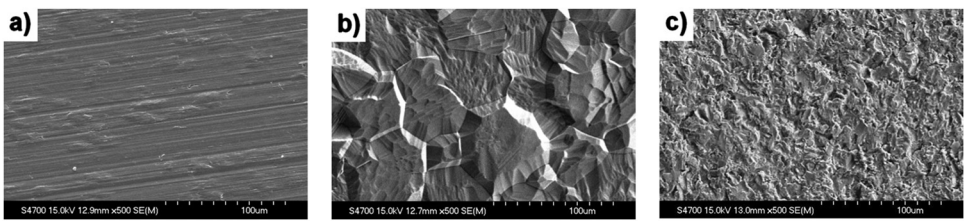

Fig. 1 SEM images of surface of titanium substrate after surface-treatment: (a) grinding, (b) etching, (c) blasting.

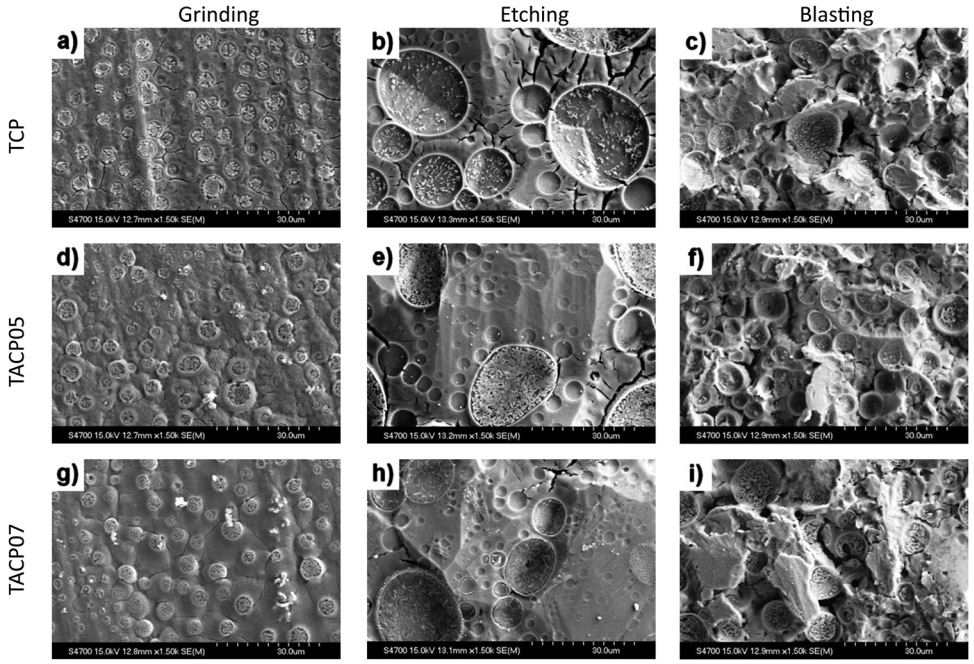

Fig. 2 SEM images of fired coatings surfaces.

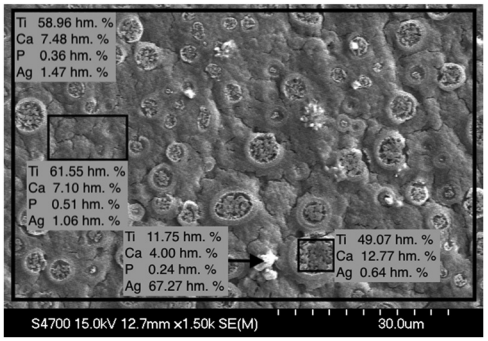

Fig. 3 Representative samples of the coating (TACP05 – grinding) with EDS analysis showing the distribution of selected major elements across the surface.

Small white spherical silver particles could be observed in the images of coatings prepared from silver-containing sols. These particles were present in the coatings both individually and in clusters. Once again, the distribution of silver particles across the coating surface was influenced by the substrate's morphology. Samples with coatings on chemically treated substrates exhibited a more even distribution of Ag particles.

Surface morphology

The roughness profiles of mechanically and chemically treated substrates are shown in Fig. 4 on the left side. Grinded samples exhibit a very uniform surface morphology, with only minor peaks visible compared to etched and blasted samples. The surface roughness of the substrate treated in an HF solution varies significantly, with abrupt changes, and average maximum and minimum values (from triplicate) of profile are (7206 ± 1.701) μm and (−8148 ± 2.468) μm. The blasted substrate surface is also highly uneven, with average values of (7691 ± 0.442) μm and (−9984 ± 0.365) μm. Compared to blasted substrates, etched ones have more flat areas. The key profile parameters are shown in Table 1.

From the roughness profiles (Fig. 4), it was evident that applying the coating to both mechanically and chemically treated substrates led to a reduction in the overall profile height. The distinctive features of the profiles (peaks, valleys, ruggedness) remained preserved even after application and firing, suggesting that the coatings replicate the relief of the surface-treated substrates quite well.

Adhesion

The surfaces of the coatings after the *tape test* are shown in Fig. 5a–i. It can be observed that the adhesion of the coatings to the surface-treated substrates was very good. The extent of the peeled coating area ranged from 0 to 5%, corresponding to classification grade 5B. None of the coatings experienced any significant damage. Only small particles of the coatings were detached at the edges of the cuts. However, these particles, along with the cracks in the coatings, had no impact on the overall test results. After the *tape test*, coatings of all types retained both the ''craters'' with calcium particles, and silver particles.

Antibacterial tests

The results of the antibacterial tests (Fig. 6) indicated consistent trends across all tested samples. In the case of the 4-hour interactions, both coatings containing silver exhibited nearly a

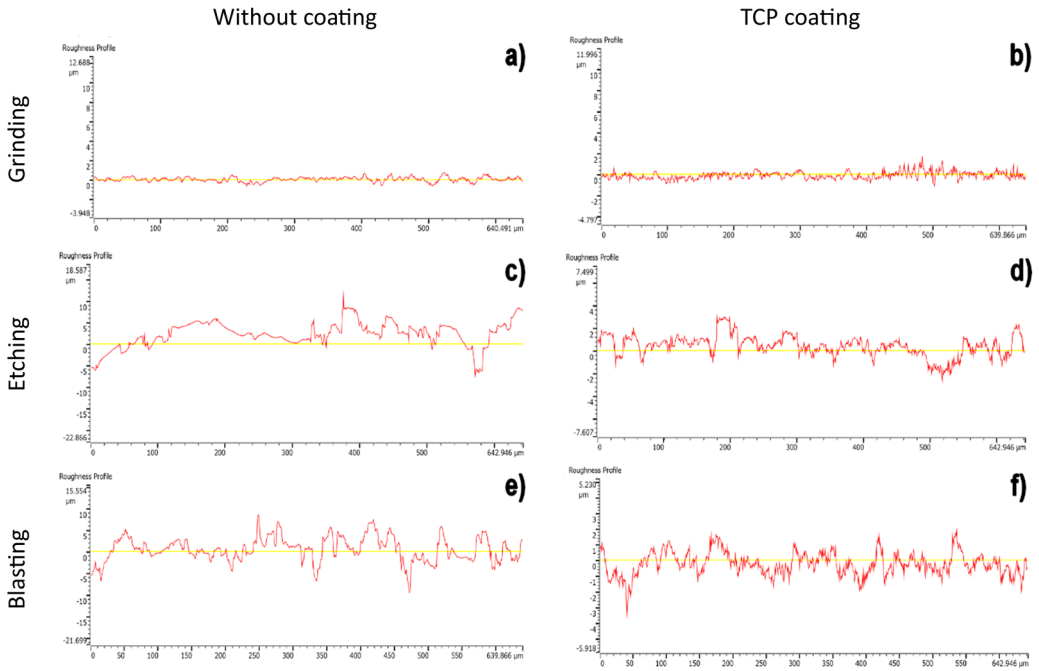

Fig. 4 Roughness profiles of mechanically and chemically treated substrates without coating and with TCP coating.

Table 1 Average values of surface profile roughness parameters in μm

	Grinding	Etching	Blasting	Grinding TCP	Etching TCP	Blasting TCP
Rp	0.599 ± 0.106	7.206 ± 1.701	7.691 ± 0.442	1.492 ± 0.331	2.864 ± 0.382	2.114 ± 0.186
Rv	0.812 ± 0.090	8.148 ± 2.468	9.984 ± 0.365	1.353 ± 0.192	3.441 ± 1.060	2.883 ± 0.548
Rt	1.411 ± 0.121	15.354 ± 4.104	17.675 ± 0.688	2.828 ± 0.204	6.305 ± 1.038	4.997 ± 0.496

Rp represents maximum profile peak height, Rv represents maximum profile valley depth, and Rt represents total height of profile.

hundred percent antibacterial efficacy. Coatings without silver showed only partial bacterial reduction. After the 24-hour interaction, the bacterial reduction for all three types of coatings was 100%, indicating an increased antibacterial effect for TCP coatings with longer interaction time.

Bioactivity

Static *in vitro* bioactivity test. Fig. 7a–i show SEM images of coatings surfaces after the 20-day static *in vitro* test of bioactivity. New phases of calcium phosphate, probably hydroxyapatite (HA, $Ca_{10}(PO_4)_6(OH)_2$), which is a mark of bioactive properties, precipitated on the surfaces of all types of samples. Precipitates occurred mainly in the places of original Ca-P ''craters''. The coatings cracks didn't have any influence on the forming of new phases. It is possible to observe small and large clusters of precipitated Ca-P growing over the circular ''craters'' and through the coating's cracks. In the images (Fig. 7d–i) of coatings with the addition of silver, silver particles are also visible, and their clusters that remained intact after the *in vitro* test.

Clusters of calcium carbonate ($CaCO_3$) can be observed in Fig. 7i. Its presence was confirmed by XRD (Supplement Ia–c, ESI†) analysis which also confirmed the presence of a small amount of hydroxyapatite (HA, $Ca_{10}(PO_4)_6(OH)_2$). Due to the small amount of precipitated Ca-P phases, it wasn't possible to perform XRD analysis on the other samples (Fig. 7a, b, d, e, g and h).

Static-dynamic *in vitro* bioactivity test. The images of the coatings surface after the bioactivity test under the static-dynamic are shown in Fig. 8a–i. Newly precipitated phases were found to be present on all tested samples. The XRD analyses (Supplement Id–i, ESI†) confirmed the presence of calcite ($CaCO_3$), which is a precursor to the formation of hydroxyapatite, on all etched (Fig. 8b, e and h) and blasted samples (Fig. 8c, f and i). As in the previous static test, the precipitates grew mainly in places of Ca-rich ''craters'', from which they spread to the surroundings and through cracks. In the case of coatings with a silver content (Fig. 8d–i), silver particles did not disappear even after 20-day of interaction with SBF.

Cytotoxicity

Non-contact test. Fig. 9 shows the results of the relative metabolic activity of the one-day long cytotoxicity test on extracts with the L929 cell line. None of the tested extracts

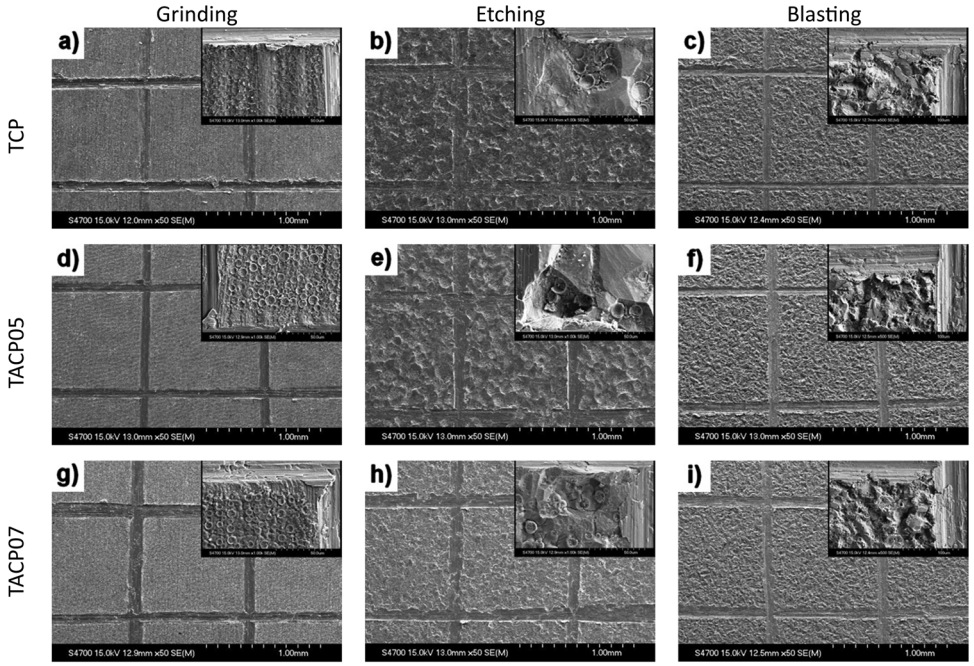

Fig. 5 SEM images of surfaces of the coatings after tape test.

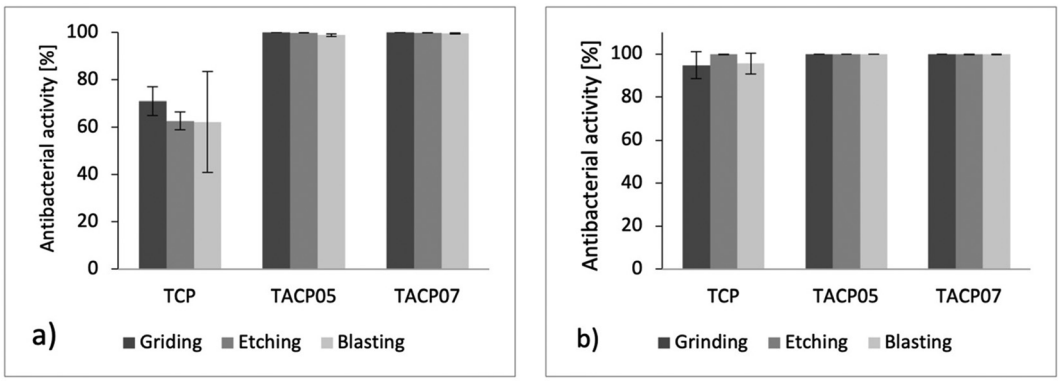

Fig. 6 Average antibacterial activity after (a) 4 hours, (b) 24 hours.

caused a decrease below the normative toxicity limit (70%). Silver concentrations in the extracts (Table 2) varied depending on the surface treatment, with the highest concentration observed in the grinding TACP07 samples. However, these levels of silver did not lead to a significant reduction in cell viability, suggesting minimal cytotoxic impact on L929 mouse fibroblast cells. Based on these results, it can be said that silver affected the viability of L929 mouse fibroblast cells only minimally, and that none of the tested coatings were toxic to these cells.

Contact test. Cell lines U-2 OS and hFOB 1.19 were chosen for direct cytotoxicity test due to their similarity to bone cells. Fig. 10 and 11 show the cytotoxicity results of the U-2 OS cell line and Fig. 12 and 13 show results of the hFOB 1.19 cell line.

The graphical representation of the relative metabolic activity of U-2 OS cells growing one day in direct contact with materials (Fig. 10) shows that the metabolic activity of grinded and etched substrates with the coating TACP07 was below the 70% viability of the control. An unexpected finding was that the same occurred in the case of the substrate treated by blasting without any coating, but other blasted samples with coatings TCP and TACP07 had a good metabolic activity (90–100%).

Fig. 11a–i show the morphology of U-2 OS cells growing on the surface-treated substrates without coatings and with TCP and TACP07 coatings observed by fluorescence microscope. Cell nuclei are coloured blue, and actin filaments are coloured red in the images. When cells are spread out, they display a healthy morphology (Fig. 11a–f, i). Cells growing on substrates (Fig. 11g and h) treated by grinding and by etching in hydrofluoric acid and coated by TACP07 appeared rounder and shrunken, indicating reduced viability. Surprisingly, the samples with a blasted substrate and a TACP07 coating, despite the

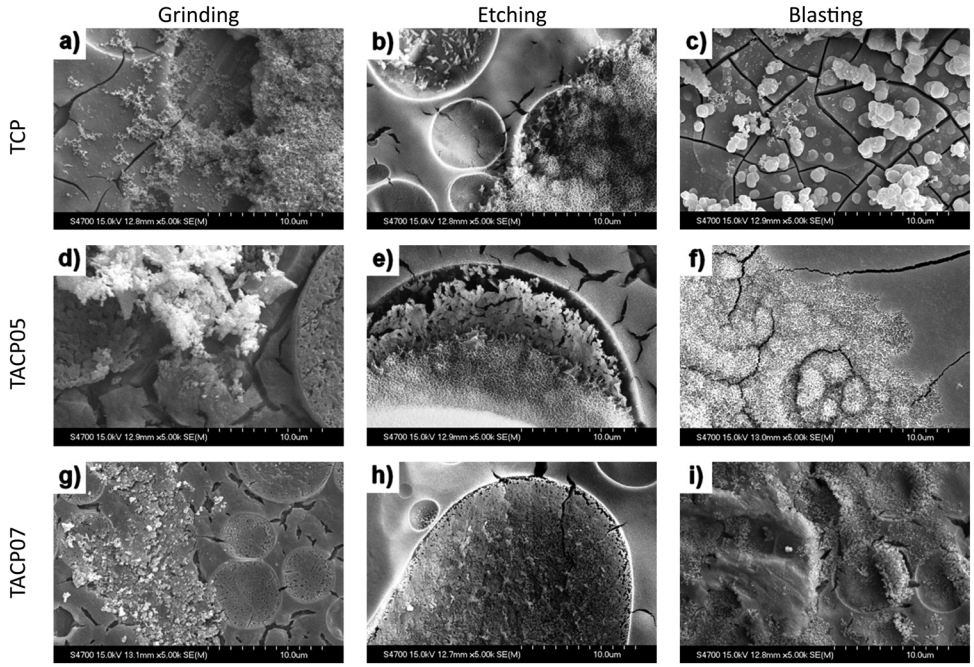

Fig. 7 SEM images of coatings surfaces after the static bioactivity test.

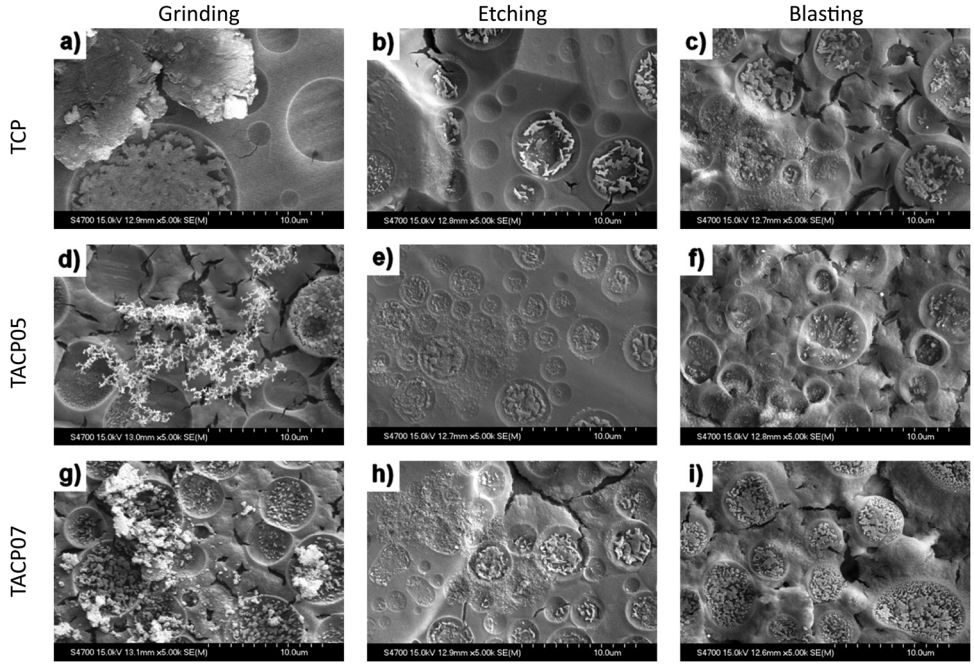

Fig. 8 SEM images of coatings surfaces after the static-dynamic bioactivity test.

silver content, achieved results comparable to samples with no coating and those with a coating without silver.

Fig. 12 graphically represents the relative metabolic activity of the hFOB 1.19 cell line after a one-day long direct toxicity test. The reduction of metabolic activity close to the toxicity limit (70%) occurred only in cases of treated samples with TACP07 coating – blasting 89% and grinding 75%. For HF-treated samples, the metabolic activity of the cells was even below the toxicity limit – 54%. For other tested samples, the relative metabolic activity ranged from 100% to 125%.

Fig. 13a–i show hFOB 1.19 cells growing on the substrates treated in three different ways and with a coating without silver

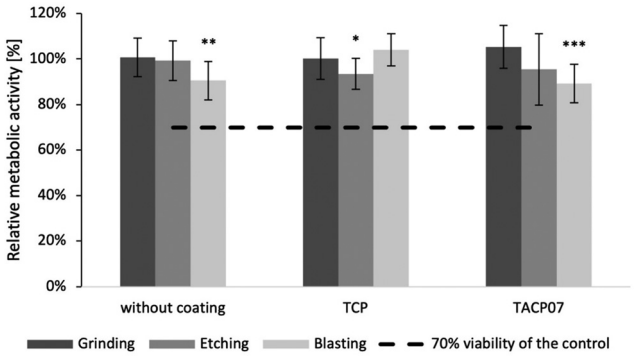

Fig. 9 Relative metabolic activity of L929 cells after one-day incubation. * indicates $p < 0.05$, ** indicates $p < 0.01$, and *** indicates $p < 0.001$.

Table 2 Silver concentration in MEM + 5% FBS extracts

Type of the coating	Ag [mg dm^{-3}]
Grinding TACP07 (1)	0.608
Grinding TACP07 (2)	0.747
Grinding TACP07 (3)	0.554
Etching TACP07 (1)	0.563
Etching TACP07 (2)	0.676
Etching TACP07 (3)	0.514
Blasting TACP07 (1)	0.437
Blasting TACP07 (2)	0.398
Blasting TACP07 (3)	0.412

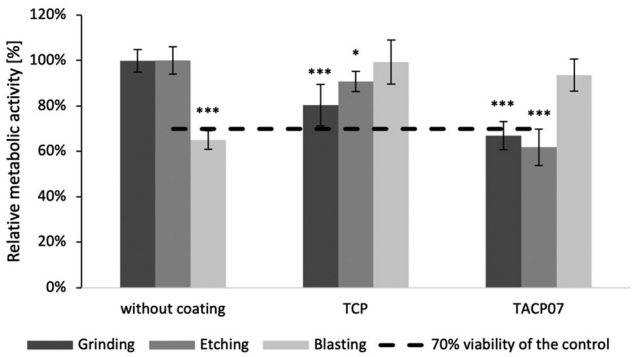

Fig. 10 Relative metabolic activity of U-2 OS cells after one-day incubation. Metabolic activity is expressed as a percentage and error bars indicate the samples standard deviation of eighteen values (three samples of each type measured in six replicates). * indicates $p < 0.05$, ** indicates $p < 0.01$, and *** indicates $p < 0.001$.

(TCP), and containing silver (TACP07). These images depict cell morphology, which reflects their viability. The best results are achieved by cells on substrates with TCP coatings lacking silver content (Fig. 13d–f). The cells are elongated, and their density is high. Rounded, thus impaired, cells are rare in images of these substrates. Cells growing on surface-treated substrates without a coating (Fig. 13a–c) exhibited poor viability, indicating unfavourable conditions for their survival. On grinded and etched samples with TACP07 coating, (Fig. 13g and h), cell density is low but most cells exhibit a typical elongated shape. An exception is a blasted sample with TACP07 coating (Fig. 13i), densely covered with live cells.

Discussion

The results of this study demonstrated that the titanium coatings containing calcium, phosphorus, and silver showed varying degrees of success depending on the specific surface treatments and the added amount of silver.

The antibacterial tests indicated that all coatings containing silver were highly effective against *Escherichia coli*, reducing bacterial growth significantly after 4 and 24 hours. This antibacterial effect was particularly strong in coatings with higher silver concentrations (c_{Ag} = 0.07 mol dm^{-3}), suggesting a dose-dependent relationship. This result underscores the potential of these coatings to prevent infections in biomedical implants, which is a critical consideration in their clinical application.

All samples also showed enhanced bioactivity in simulated body fluid (SBF), especially samples that underwent mechanical surface treatments. The increased surface roughness resulting from grinding and blasting likely provided more nucleation sites for the precipitation of new phases, thus improving osseointegration potential. On the other hand, chemically etched surfaces, despite slightly increased roughness, exhibited less uniform precipitate formation, potentially due to the irregular morphology created by the etching process. This would suggest that mechanical treatment is more effective in promoting the bioactive response leading to successful osseointegration.

The *tape test* showed that all coatings (TCP, TACP05, and TACP07) exhibited excellent adhesion to both chemically and mechanically treated titanium substrates. Strong adhesion is a critical property for biomedical applications, ensuring that the coatings remain intact and functional. This shows that these coatings are suitable for their intended use in biomaterials, particularly in applications where long-term stability and durability are important.

The cytotoxicity and cell morphology tests highlighted significant differences in cellular responses based on the type of coating, surface treatment, and testing method. Non-contact testing, where cells interact only with material extracts, is standardized but less precise, as it does not account for direct material-cell interactions. Contact testing, which involves direct contact between cells and the test material, provides stricter and more accurate results, reflecting a more realistic cellular response to the material's surface properties. In non-contact tests, no sample treatment reduced the metabolic activity of L929 cells below the normative toxicity limit (*i.e.*, below 70% of the metabolic activity of the negative control). This indicates that the materials are generally biocompatible. Although silver concentrations in the extracts varied based on surface treatment (Table 2), none reached levels sufficient to significantly reduce cell viability. This suggests that while surface treatments influence the release of silver, the concentrations observed in

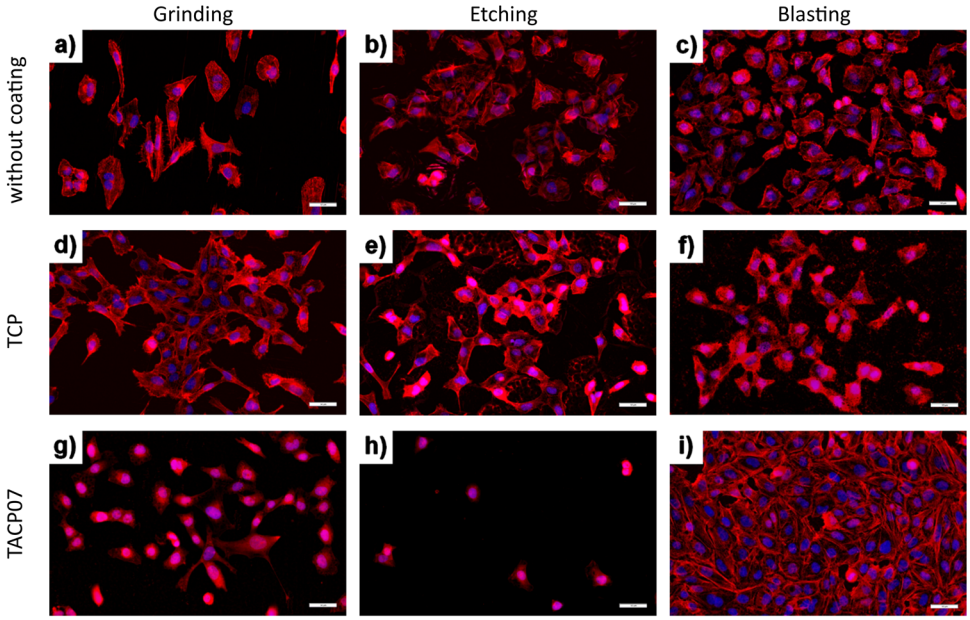

Fig. 11 Images of U-2 OS cells growing on the substrates surface.

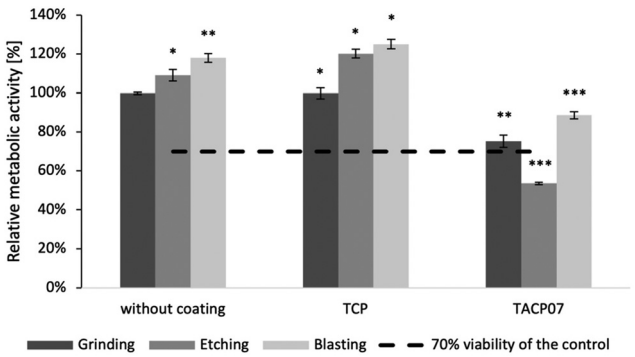

Fig. 12 Relative metabolic activity of hFOB 1.19 cells after one-day incubation. Metabolic activity is given as a percentage (control – ground titanium – represent 100%) Error bars represent the relative standard deviation of the three values. * indicates $p < 0.01$, ** indicates $p < 0.001$, and *** indicates $p < 0.0001$.

this study were not high enough to induce cytotoxic effects in non-contact tests, aligning with the observed minimal cytotoxicity in L929 cells (Fig. 9). For uncoated substrates, both U-2 OS and hFOB 1.19 cells generally exhibited high metabolic activity in contact tests (except the blasted substrate with U-2 OS cells) (Fig. 10 and 12). Healthy morphology was observed in U-2 OS cells on all surface treatments (Fig. 11a–c). The cells were well spread out, suggesting that the uncoated titanium surface provides a supportive environment for cell attachment and growth. In, contrast, hFOB cells showed poor viability on these substrates because they were few and rounded (Fig. 13a–c). When comparing the cell metabolic activity results with the images of the cells growing on the surface of the samples, a discrepancy can be observed on the blasted uncoated substrate with U-2 OS cells (Fig. 10 and 11c). According to the metabolic activity results, which may have been reduced due to residual aluminium from the blasting process, there should have been a reduction in the number of cells. However, the images showed that a relatively large number of cells were present on the substrate, and they had a healthy morphology (Fig. 11c). For substrates coated with TCP (without silver), the results were more favourable. U-2 OS and hFOB 1.19 cells on these substrates generally exhibited better viability than uncoated substrates, with cells spreading out and maintaining a healthy morphology (Fig. 10, 11d–f, 12, and 13d–f). This suggests that the TCP coating provides a more supportive environment for cell growth than the uncoated titanium, likely due to the coating's ability to enhance surface properties without introducing cytotoxic elements. In contrast, the substrates coated with TACP07 (higher silver concentration) exhibited reduced cell viability in contact tests. On the chemically treated and grinded substrates with TACP07 coating, both U-2 OS and hFOB 1.19 cells showed significantly lower viability (Fig. 10, 11g, h, 12 and 13g, h). The cells often appeared rounded, indicating poor attachment. This reduced viability is likely due to the cytotoxic effects of silver ions released from the coatings. However, a surprising finding was observed on the blasted substrate with TACP07 coating (Fig. 11i and 12i), where both U-2 OS and hFOB 1.19 cells exhibited relatively high viability and healthy morphology. Both the metabolic activity and the images of the cells indicated that the cells were growing on this surface, despite the uneven surface and the presence of silver.

These variations in cell viability could be attributed to the differences in surface roughness and chemical composition introduced by the treatments, which are known to influence cell attachment and proliferation. One potential reason for the lower cell viability on certain samples could be the presence of

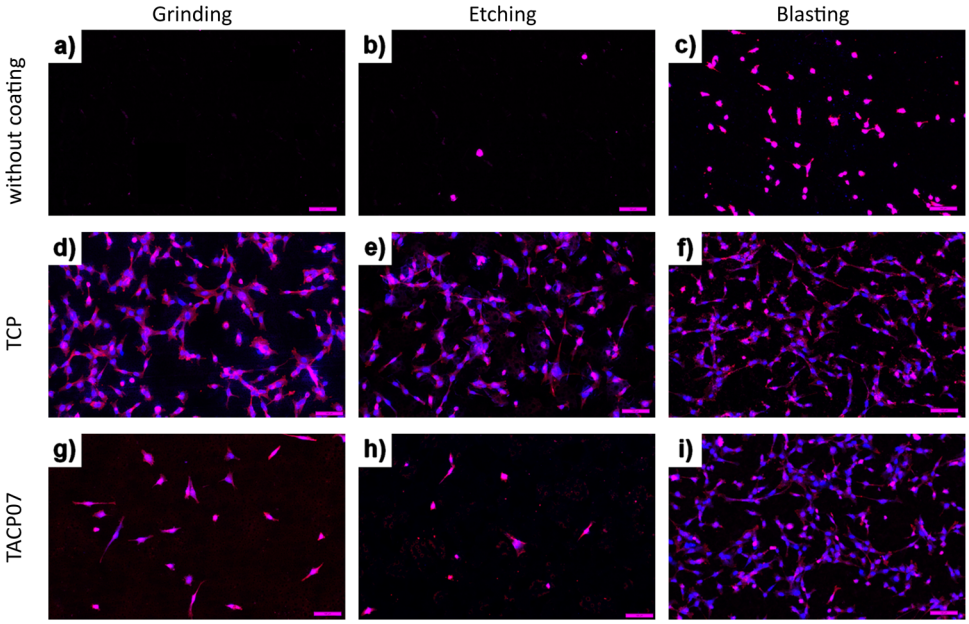

Fig. 13 Images of hFOB 1.19 cells growing on the substrates surface.

residual stress or suboptimal surface morphology, which may create an unfavourable environment for cell growth. Additionally, the distribution and concentration of silver ions likely contributed to cytotoxic effects in some coatings especially with higher content of silver, highlighting the need for precise control over the incorporation of antibacterial agents.

These results are consistent with other studies showing that surface roughness and chemical composition can significantly affect bioactivity and cell compatibility of coatings on titanium implants.[2–4] Previous research has also found that rough surface textures, especially those created by mechanical treatments like grinding and blasting, help improve osseointegration by providing more sites for nucleation.[35–37] However, unlike other studies, this work offers a direct comparison of multiple surface treatments, giving new insights into how each one affects antibacterial properties, cell viability, and bioactivity. By investigating the combined effects of silver, calcium, and phosphorus, this study adds to current knowledge with a broader understanding of how multifunctional coatings perform on titanium surfaces.

The different behaviour of the coatings can be attributed to the specifics of the surface treatments:

•Grinding: produced a uniform rough surface, offering consistent nucleation sites for precipitation, enhancing coating adhesion, and did not adversely affect cytocompatibility. Unlike blasting or chemical etching, grinding does not introduce residual chemicals or foreign particles that could negatively impact cell viability.

•Blasting: created a highly fragmented surface with significant height variations, which might have induced stress and cracking in the coatings. This could affect the distribution and efficacy of bioactive and antibacterial components, and the residue from the blasting process may also impact cytocompatibility, potentially leading to less favourable interaction with cells.

•Chemical etching: resulted in a highly irregular surface morphology with abrupt roughness changes, potentially leading to unpredictable new phase formation. The irregular morphology and residual chemicals from the etching process could negatively affect cytocompatibility.

These findings suggest that while the multifunctional coatings hold promise for improving implant performance, careful optimization of the surface treatments is essential to balance bioactivity, antibacterial properties, and cytocompatibility. Future studies should focus on refining these parameters to develop coatings that maximize therapeutic benefits while minimizing potential adverse effects.

Conclusion

This study successfully prepared and evaluated titanium coatings containing calcium, phosphorus, and silver on chemically and mechanically modified titanium substrates. The results demonstrated that different surface treatments significantly influence the coatings' bioactivity, antibacterial properties, and cytocompatibility. Mechanical treatments, especially grinding, provided the most uniform and effective surface for bioactive and antibacterial coatings.

The inclusion of calcium and phosphorus enhanced bioactivity and potential osseointegration, while the addition of silver provided effective antibacterial action. However, samples with the higher concentration of silver exhibited cytotoxicity, highlighting the need for future optimization of the coating composition and surface treatments.

Overall, this research contributes valuable insights into the development of advanced titanium-based biomaterials with

multifunctional properties. By addressing the balance between bioactivity, antibacterial efficacy, and cytocompatibility, these findings pave the way for future studies aimed at improving the safety and effectiveness of biomedical implants.

Author contributions

Karolína Opavová: methodology; measurement; writing – original draft preparation. Diana Horkavcová: conceptualization; methodology; measurement; writing – review and editing; supervision. Eva Jablonská: conceptualization; methodology; measurement; writing – review and editing; supervision. Lucie Mrázková: measurement. Anna Bašusová: measurement.

Data availability

The data supporting this article have been included as part of the ESI.†

Conflicts of interest

There are no conflicts to declare.

Acknowledgements

This research received no external funding.

References

1 D. Manshadi, P. Yu, M. Dargusch, D. StJohn and M. Qian, *Powder Technol.*, 2020, **364**, 189–204, DOI: 10.1016/j.powtec.2020.01.073.
2 S. Bose, S. F. Robertson and A. Bandyopadhyay, *Acta Biomater.*, 2018, **66**, 6–22, DOI: 10.1016/j.actbio.2017.11.003.
3 M. Z. Ibrahim, A. A. D. Sarhan, F. Yusuf and M. Hamdi, *J. Alloys Compd.*, 2017, **714**, 636–667, DOI: 10.1016/j.jallcom.2017.04.231.
4 L. Le Guéhennec, A. Soueidan, P. Layrolle and Y. Amouriq, *Dent. Mater.*, 2007, **23**, 844–854, DOI: 10.1016/j.dental.2006.06.025.
5 O. Zinger, K. Anselme, A. Denzer, P. Habersetzer, M. Wieland, J. Jeanfils, P. Hardouin and D. Landolt, *Biomaterials*, 2004, **25**, 2695–2711, DOI: 10.1016/j.biomaterials.2003.09.111.
6 P. Usinskas, Z. Stankeviciute, A. Beganskiene and A. Kareiva, *Surf. Coat. Technol.*, 2016, **307**, 935–940, DOI: 10.1016/j.surfcoat.2016.10.032.
7 S. F. Robertson, A. Bandyopadhyay and S. Bose, *Surf. Coat. Technol.*, 2019, **372**, 140–147, DOI: 10.1016/j.surfcoat.2019.04.071.
8 G. J. Owens, R. K. Singh, F. Foroutan, M. Alqaysi, C.-M. Han, C. Mahapatra, H.-W. Kim and J. C. Knowles, *Prog. Mater. Sci.*, 2016, **77**, 1–79, DOI: 10.1016/j.pmatsci.2015.12.001.
9 M. Skolik, A. Domanowska, P. Karasiński, E. Gondek and A. Michalewicz, *Mater. Lett.*, 2019, **251**, 210–213, DOI: 10.1016/j.matlet.2019.05.071.
10 J. C. B. Alcázar, R. M. J. Lemos, M. C. M. Conde, L. A. Chisini, M. M. S. Salas, B. S. Noremberg, F. V. da Motta, F. F. Demarco, S. B. C. Tarquinio and N. L. V. Carreño, *Prog. Org. Coat.*, 2019, **130**, 206–213, DOI: 10.1016/j.porgcoat.2019.02.007.
11 Y. Ergün and M. S. Başpınar, *Int. J. Hydrogen Energy*, 2017, **42**, 20420–20429, DOI: 10.1016/j.ijhydene.2017.06.051.
12 M. Catauro, F. Papale and F. Bollino, *Mater. Sci. Eng., C*, 2016, **58**, 846–851, DOI: 10.1016/j.msec.2015.09.033.
13 Z. Chen, K. Zhou, X. Lu and Y. A. Cheong Lam, *Acta Mech.*, 2014, **225**, 431–452, DOI: 10.1007/s00707-013-0979-y.
14 W. S. W. Harun, R. I. M. Asri, J. Alias, F. H. Zulkifli, K. Kadirgama, S. A. C. Ghani and J. H. M. Shariffuddin, *Ceram. Int.*, 2018, **44**, 1250–1268, DOI: 10.1016/j.ceramint.2017.10.162.
15 C. Magdaleno-López and J. de Jesús Pérez-Bueno, *Int. J. Adhes. Adhes.*, 2020, **98**, 102551, DOI: 10.1016/j.ijadhadh.2020.102551.
16 W. Zai, C. L. Wu and H. C. Man, *Mater. Lett.*, 2020, **270**, 127696, DOI: 10.1016/j.matlet.2020.127696.
17 G. Womack, K. Isbilir, F. Lisco, G. Durand, A. Taylor and J. M. Walls, *Surf. Coat. Technol.*, 2019, **358**, 76–83, DOI: 10.1016/j.surfcoat.2018.11.030.
18 M. Tiskaya, S. Shahid, D. Gillam and R. Hill, *Dent. Mater.*, 2021, **37**, 296–310, DOI: 10.1016/j.dental.2020.11.015.
19 C. Mocquot, N. Attik, N. Pradelle-Plasse, B. Grosgogeat and P. Colon, *Dent. Mater.*, 2020, **36**, 1116–1143, DOI: 10.1016/j.dental.2020.03.020.
20 International Organization for Standardization, 2014, Implants for Surfery: In Vitro Evaluation for Apatite-Forming Ability of Implant Materials (ISO Standard No. 23317:2014), https://www.iso.org/standard/65054.html.
21 V. Krishnan and D. Lakshmi, *J. Adv. Pharm. Technol. Res.*, 2013, **4**, 78–83, DOI: 10.4103/2231-4040.111523.
22 V. A. Ponomarev, E. A. Orlov, N. A. Malikov, Y. V. Tarasov, A. N. Sheveyko, E. S. Permyakova, K. A. Kuptsov, I. A. Dyatlov, S. G. Ignatov, A. S. Ilnitskaya, N. A. Gloushankova, B. Subramanian and D. V. Shtansky, *Appl. Surf. Sci.*, 2020, **516**, 146068, DOI: 10.1016/j.apsusc.2020.146068.
23 K. Batebi, B. Abbasi Khazaei and A. Afshar, *Surf. Coat. Technol.*, 2018, **352**, 522–528, DOI: 10.1016/j.surfcoat.2018.08.021.
24 M. S. Zafar, I. Farooq, M. Awais, S. Najeeb, Z. Khurshid and S. Zohaib, *Biomed., Ther. Clin. Appl. Bioact. Glasses*, 2019, 313–329, DOI: 10.1016/B978-0-08-102196-5.00011-2.
25 M. Aftab, M. Z. Butt, D. Ali, F. Bashir and Z. H. Aftab, *Ceram. Int.*, 2020, **46**, 5037–5049, DOI: 10.1016/j.ceramint.2019.10.247.
26 N. Cotolan, M. Rak, M. Bele, A. Cör, L. M. Muresan and I. Milošev, *Surf. Coat. Technol.*, 2016, **307**, 790–799, DOI: 10.1016/j.surfcoat.2016.09.082.
27 Y. Xiang, J. Li, X. Liu, Z. Cui, X. Yang, K. W. K. Yeung, H. Pan and S. Wu, *Mater. Sci. Eng., C*, 2017, **79**, 629–637, DOI: 10.1016/j.msec.2017.05.115.
28 D. Horkavcová, P. Novák, I. Fialová, M. Černý, E. Jablonská, J. Lipov, T. Ruml and A. Helebrant, *Mater. Sci. Eng. C*, 2017, **76**, 25–30, DOI: 10.1016/j.msec.2017.02.137.
29 C. G. Anjali Das, V. Ganesh Kumar, T. Stalin Dhas, V. Karthick, K. Govindaraju, J. Mary Joselin and J. Baalamurugan, *Biocatal. Agric. Biotechnol.*, 2020, 101593, DOI: 10.1016/j.bcab.2020.101593.
30 C. Sun, W. Zhang, R. Ding, J. Wang and L. Yao, *Chemosphere*, 2020, **253**, 126705, DOI: 10.1016/j.chemosphere.2020.126705.
31 E. S. Istifli, M. T. Hüsunet and H. B. Ila, Cytotoxicity - Definition, Identification, and Cytotoxic Compounds, IntechOpen, 2019, DOI: 10.5772/intechopen.88368.

32 L. Ghasemi-Mobarakeh, D. Kolahreez, S. Ramakrishna and D. Williams, *Curr. Opin. Biomed. Eng.*, 2019, **10**, 45–50, DOI: 10.1016/j.cobme.2019.02.004.
33 W. Li, J. Zhou and Y. Xu, *Biomed. Rep.*, 2015, **3**, 617–620, DOI: 10.3892/br.2015.481.
34 F. Heidenau, W. Mittelmeier, R. Detsch, M. Haenle, F. Stenzel, G. Ziegler and H. Gollwitzer, *J. Mater. Sci.: Mater. Med.*, 2005, **16**, 883–888, DOI: 10.1007/s10856-005-4422-3.
35 E. Borshcheva, D. Horkavcová, Z. Cílová and A. Helebrant, *Ceram.-Silik.*, 2011, **55**, 331–336.
36 L. Le Guehennec, E. Goyenvalle, M.-A. Lopez-Heredia, P. Weiss, Y. Amouriq and P. Layrolle, *Clin. Oral. Implants Res.*, 2008, **19**, 1103–1110, DOI: 10.1111/j.1600-0501.2008.01547.x.
37 K. Švagrová, D. Horkavcová, E. Jablonská and A. Helebrant, *J. Biomed. Mater. Res., Part B*, 2022, **110**, 115–124, DOI: 10.1002/jbm.b.34895.